GAMMA IRRADIATION IN JSI TRIGA REACTOR

KLEMEN AMBROŽIČ [1], VLADIMIR RADULOVIĆ [1] and LUKA SNOJ[1]

[1] *F8, Reactor physics department, "Jožef Stefan" Institute, Jamova cesta 39, SI-1000 Ljubljana, Slovenia*

Abstract

The "Jožef Stefan" Institute (JSI) TRIGA mk. II (TRIGA) reactor irradiation facilities have been throughout it's 50 years of operation, extensively used for neutron irradiation of samples, from neutron activation analysis, radiation hardness studies and electronic component testing. Recently there has been an increased interest in high dose-rate pure γ irradiations. Activated JSI TRIGA fuel elements are being utilized as both in-core γ source for irradiation in the existing irradiation positions, as well as a source for a new ex-core irradiation facility. The new facility consists of 6 TRIGA fuel elements stacked into a fuel rack at the edge of the reactor tank, and an aluminium box (inner dimensions $30\,\mathrm{cm}\times20\,\mathrm{cm}\times20\,\mathrm{cm}$) submerged in close proximity of the activated fuel, with a cable guide tube, submerged to close proximity of the activated fuel. During the irradiation, the dose-rate field is monitored using a gas flow ionization chamber, with maximum dose rates reaching $100\,\mathrm{Gy\,h^{-1}}$.
In this paper, the characterization of the prompt γ field in the existing, as well as the delayed γ field in the new irradiation facility is presented, performed both computationally and by γ dose rate measurements. The goal is to characterize the γ field in the JSI TRIGA irradiation positions γ field, in order to provide an adequate γ field description in terms of the γ flux and spectrum, in order to qualify the response of the samples under irradiation.

1 Introduction

Electronic equipment inside commercial fission reactor plants is subjected to intermediate levels of irradiation [1], predominantly by γ rays produced during fission, activation of primary coolant water [2] or from neutron activation γ rays after reactor shutdown [3]. Electronic devices inside a commercial nuclear power plant (NPP) containment building must maintain their uninterrupted operation between outages and even in accident scenario cases. Therefore, radiation tolerant systems must be installed inside the containment building. Radiation tolerance tests of electronic components and assemblies are usually performed in ^{60}Co and ^{137}Cs irradiation facilities, with γ-ray energies of $1.17\,\mathrm{MeV}$, $1.33\,\mathrm{MeV}$ and $661.6\,\mathrm{keV}$ respectively. However γ-rays, emitted from activated nuclear fuel and primary water activation inside a NPP have energies up to $10\,\mathrm{MeV}$. Therefore, it is desirable to test the equipment in a γ field with representative energies [4], i.e. reactor fuel spectrum.

The "Jožef Stefan" Institute (JSI) TRIGA mk. II (TRIGA) reactor is a $250\,\mathrm{kW}$ pool type, reactor, with U-ZrH fuel elements, equipped with several irradiation positions, which in its 50 years of operation have commonly been utilized for neutron irradiation of samples, the possibility of irradiations with γ rays only has however not been explored in depth. Several dry irradiation positions can be inserted directly into the reactor core (in-core) into fuel element positions (outer diameter $3.76\,\mathrm{cm}$) with the exception of a larger Triangular channel (TriC), which occupies 3 fuel element positions. There are also 40 cylindrical irradiation positions in a rotary carousel outside the reactor core graphite reflector, into which

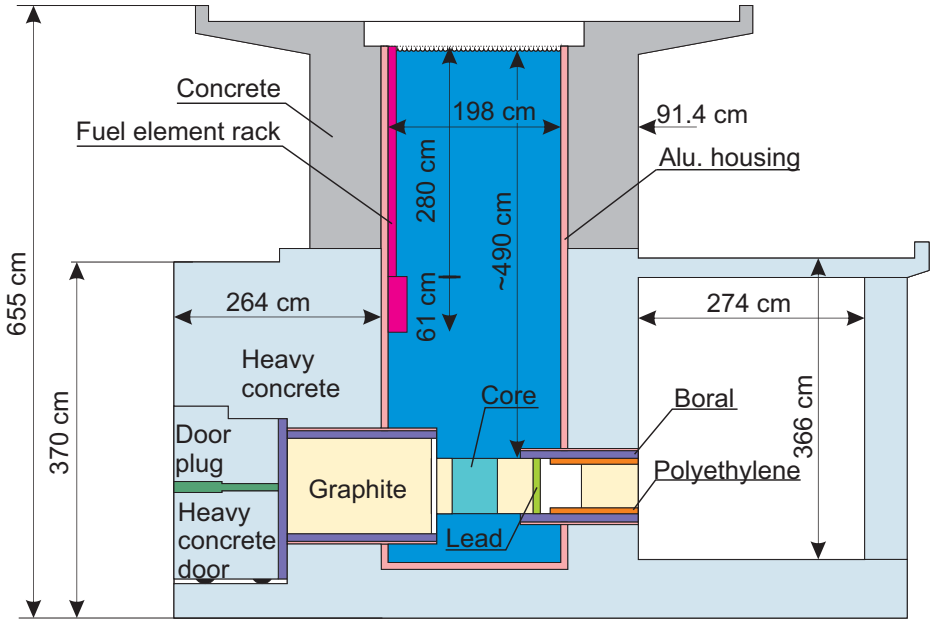

Figure 1: Side-view schematic of the JSI TRIGA reactor.

capsules $5.34\,\mathrm{cm}$ long and $2.4\,\mathrm{cm}$ in diameter can be inserted. There are also 3 larger horizontal irradiation ports with inner diameter of $15\,\mathrm{cm}$ and centerline height $9.4\,\mathrm{cm}$ below reactor core center. The neutron field in these irradiation positions has been thoroughly computationally characterized [5], and results validated by measurements [6]. Due to the neutron characterization, JSI TRIGA has become a reference center for neutron irradiation of detectors for ATLAS experiment, CERN [7] in the framework of AIDA II project.
Above-mentioned irradiation facilities can also be used for γ irradiations in a mixed field during reactor operation and in a pure γ field after reactor shutdown, with activated nuclear fuel decaying, emitting high energy γ rays. In this regard, the γ field can be divided into two distinct parts: prompt γ rays, which are emitted promptly after a reaction of neutron with nucleus, and delayed γ rays, which are emitted due to the radioactive decay of neutron activated nuclei. Computational characterization of prompt γ field inside existing irradiation facilities has been performed, utilizing ambient dose ICRP-21 [8] and ANSI-ANS6.1.1.1977 [9] flux to dose conversion factors (fig. 3) and air kerma rate calculations. Measurements of miniature ionization chamber currents in the JSI TRIGA reactor demonstrate the importance of the delayed contribution to the photon field in nuclear reactors, contributing $30\,\%$ to the total γ field flux [10]. A γ measurement campaign in collaboration with the French Commissariat à l'ènergie et aux ènergies alternatives (CEA) and Polish Nuclear Institute Krakow (IFJ) is currently under way for γ field characterization, with emphasis on prompt and delayed γ discrimination. A novel generalized Rigorous-2-Step (R2S) [11] delayed γ field computational modeling approach code is also under development for delayed γ field characterization of irradiation facilities, which will be validated by the measurement data.

For whole electronic assemblies, the size of existing irradiation facilities poses a limiting factor, and were not designed with the thought of having electronic cables attached to the samples. Therefore a new larger, detachable, ex-core irradiation facility consisting of a watertight aluminum box with internal dimensions of $30\,\mathrm{cm} \times 20\,\mathrm{cm} \times 20\,\mathrm{cm}$ with a long cable guide tube leading to the reactor platform was constructed, utilizing 6 activated reactor fuel elements stacked into a fuel element rack at the edge of a reactor tank as a delayed γ ray source. During sample irradiation, on-line dose rate monitoring inside the

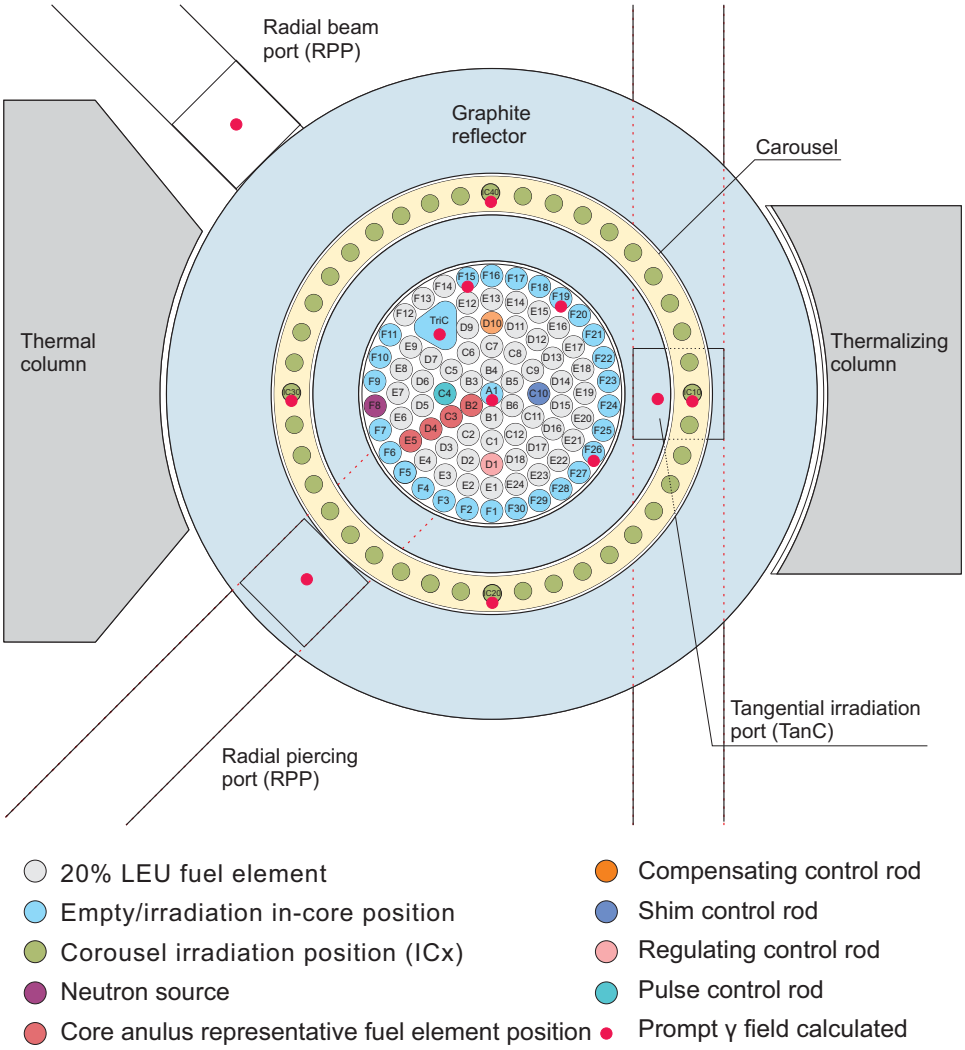

Figure 2: Schematic core view of the JSI TRIGA reactor with irradiation positions, denoted positions with prompt γ ray dose rates calculated and representative fuel elements from each core annulus for the delayed γ calculations.

irradiation box is performed by a gas flow ionization chamber, with initial dose rate measurements (immediately after shut-down) in excess of $100\,\mathrm{Gy\,h^{-1}}$. Even with increased internal dimensions of the facility, γ field gradients inside were not measured, due to its inaccessibility during irradiation and due to large dimensions of the gas flow ionization chamber. A thorough characterization still needs to be performed, using smaller detectors, such as thermo-luminescent detectors (TLDs), optically stimulated luminescent detectors (OSLDs) or radiation sensitive field effect transistors (RadFETs) [12]. In parallel , a computational analysis has been performed by per fuel element specific R2S code, to evaluate the dose-rates inside the new irradiation facilities, and to evaluate the field homogeneity with different fuel element rack filling patterns.

2 Reactor γ field

Characterization of the γ field inside reactor irradiation facilities (excluding the new irradiation box) is under way, both experimentally and computationally. With a still ongoing γ field measurement campaign and a generalized delayed γ computational code still under development, only computational prompt γ field characterization has been performed so

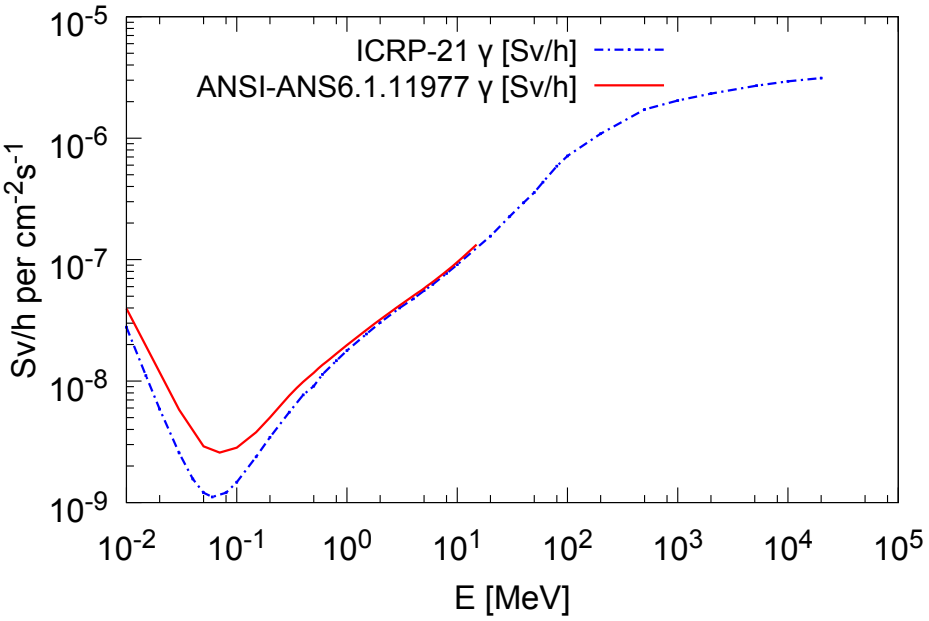

Figure 3: Flux to dose-rate ambient dose equivalent ICRP-21 and ANSI-ANS6.1.1.1977 conversion factors.

Table 1: Total prompt γ-ray air kerma and dose rate inside JSI TRIGA irradiation facilities at full reactor power (250 kW).

Channel	γ air kerma [Gy h^{-1}]	γ ICRP-21 [Sv h^{-1}]	γ ANS6 [Sv h^{-1}]
RPP	$2.87 \times 10^4(1 \pm 4 \times 10^{-4})$	$3.17 \times 10^4(1 \pm 4 \times 10^{-4})$	$3.66 \times 10^4(1 \pm 4 \times 10^{-4})$
RBP	$2.64 \times 10^3(1 \pm 2 \times 10^{-3})$	$2.92 \times 10^3(1 \pm 2 \times 10^{-3})$	$3.31 \times 10^3(1 \pm 2 \times 10^{-3})$
TanC	$2.14 \times 10^4(1 \pm 5 \times 10^{-4})$	$2.36 \times 10^4(1 \pm 5 \times 10^{-4})$	$2.74 \times 10^4(1 \pm 5 \times 10^{-4})$
A1	$2.91 \times 10^5(1 \pm 3 \times 10^{-4})$	$3.25 \times 10^5(1 \pm 3 \times 10^{-4})$	$3.66 \times 10^5(1 \pm 3 \times 10^{-4})$
TriC	$1.68 \times 10^5(1 \pm 3 \times 10^{-4})$	$1.88 \times 10^5(1 \pm 3 \times 10^{-4})$	$2.12 \times 10^5(1 \pm 3 \times 10^{-4})$
IC10	$1.68 \times 10^4(1 \pm 1 \times 10^{-3})$	$1.87 \times 10^4(1 \pm 1 \times 10^{-3})$	$2.11 \times 10^4(1 \pm 9 \times 10^{-4})$
IC20	$1.63 \times 10^4(1 \pm 1 \times 10^{-3})$	$1.82 \times 10^4(1 \pm 1 \times 10^{-3})$	$2.06 \times 10^4(1 \pm 1 \times 10^{-3})$
IC30	$1.64 \times 10^4(1 \pm 1 \times 10^{-3})$	$1.83 \times 10^4(1 \pm 1 \times 10^{-3})$	$2.07 \times 10^4(1 \pm 1 \times 10^{-3})$
IC40	$1.69 \times 10^4(1 \pm 1 \times 10^{-3})$	$1.89 \times 10^4(1 \pm 1 \times 10^{-3})$	$2.13 \times 10^4(1 \pm 9 \times 10^{-4})$
F15	$9.16 \times 10^4(1 \pm 3 \times 10^{-4})$	$1.02 \times 10^5(1 \pm 3 \times 10^{-4})$	$1.16 \times 10^5(1 \pm 3 \times 10^{-4})$
F19	$8.26 \times 10^4(1 \pm 3 \times 10^{-4})$	$9.25 \times 10^4(1 \pm 3 \times 10^{-4})$	$1.05 \times 10^5(1 \pm 3 \times 10^{-4})$
F26	$8.40 \times 10^4(1 \pm 3 \times 10^{-4})$	$9.40 \times 10^4(1 \pm 3 \times 10^{-4})$	$1.07 \times 10^5(1 \pm 3 \times 10^{-4})$

far, using the Monte Carlo MCNP6 v.1 code [13] and ENDF/B VII.0 nuclear data library [14]. The computational model is based on the criticality benchmark experiment model [15], with additional fuel holding pin, top and bottom reactor core fuel holding grate and neutron instrumentation details.

Due to the nature of prompt γ generation, the field is proportional to the reactor power. In table 1 ambient dose equivalents using ICRP-21 and ANSI-ANS6.1.1.1977 flux to dose conversion factors and air kerma rates inside reactor irradiation facilities 2 is calculated at full reactor power (250 kW) along with their 1σ statistical uncertainty. Ambient dose equivalent fields inside the reactor core at fuel element center height (fig. 4a) and at horizontal irradiation positions center height (fig. 4b) have also been calculated. We can observe that the dose rates are quite significant, spanning from 3×10^3 Gy h^{-1} to 4×10^5 Gy h^{-1} or Sv h^{-1}. We must keep in mind that the delayed part of the γ field if still missing, con-

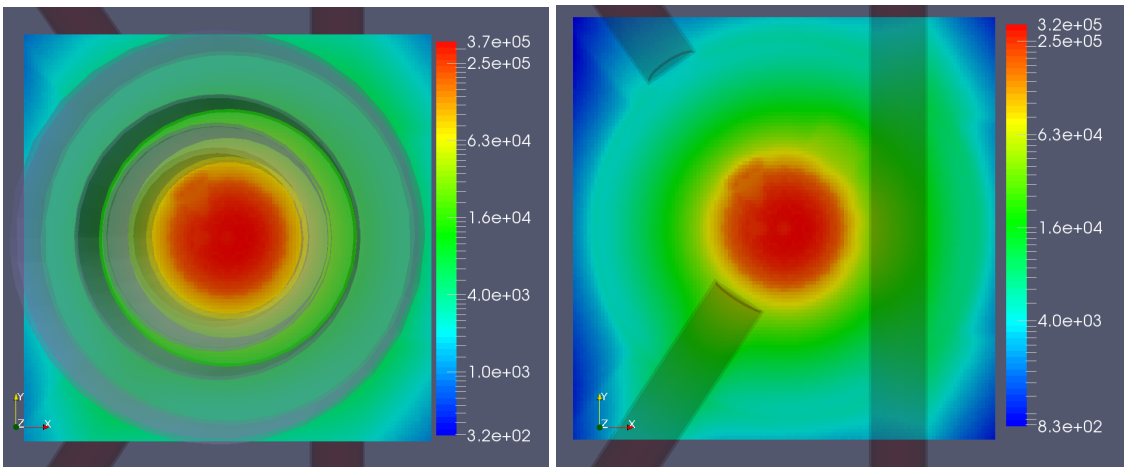

(a) Ambient dose rate equivalent at fuel element center height.

(b) Ambient dose rate equivalent at horizontal irradiation position center height.

Figure 4: ICRP-21 H*10 γ ambient dose equivalent rate field at full reactor power (250 kW)

tributing roughly 30 % [10]. During reactor operation a neutron field of the same order of magnitude also exists inside the respective irradiation positions.
The above computational results also provide valuable information for experimental campaign, with γ-ray field intensities spanning over 6 orders of magnitude, reaching over 1×10^2 kGy h^{-1} or over 1×10^2 kSv h^{-1}. This limits the choice of detectors which can withstand such high levels of radiation and have appropriate measurement ranges to ionization chambers and TLDs, using novel readout techniques [16].

3 New irradiation facility

The new irradiation facility was constructed to accommodate larger electronic assemblies for pure γ irradiation, which need to be tested at large dose-rates and to large to fit inside the existing irradiation positions. 6 fuel elements were transfered into the fuel element rack, positioned at the edge of the reactor tank. This provided a viable γ source, with initial dose-rate measurements in excess of 100 Gy h^{-1} in close proximity. However these measurements were not performed under controlled conditions and further investigation is required.

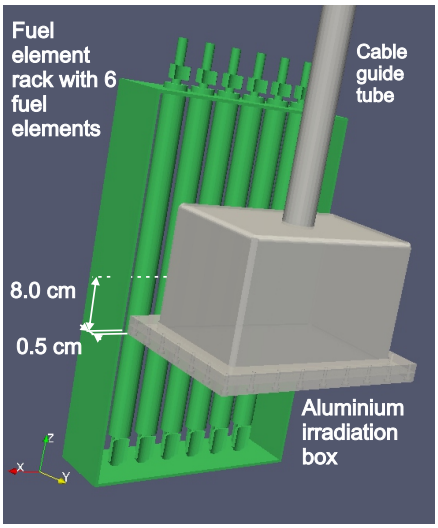

Figure 5: Schematic of the simulation model. Concrete wall behind the fuel rack.

An irradiation box, made of 5 mm thick aluminum, with a removable backplate for sample insertion and a cable guide tube for sample and dose-rate monitoring equipment was constructed, with inner dimensions of 30 cm × 20 cm × 20 cm. This enabled irradiations of larger electronic assemblies, and to test integral assembly radiation hardness.

The irradiation position is inaccessible during the irradiation and therefore it is impossible to manipulate the gas flow ionization chamber position to measure gamma field gradients. Another set of measurements under controlled conditions is planned in the near future, utilizing TLDs for dose field mapping inside the irradiation box. In the meantime, a representa-

tive Monte Carlo MCNP computational model was constructed, utilizing delayed 22-group delayed γ spectra and intensities of fuel elements from each core annulus, irradiated for 1 h, by the R2S methodology [3], in order to asses the γ intensity and homogeneity.

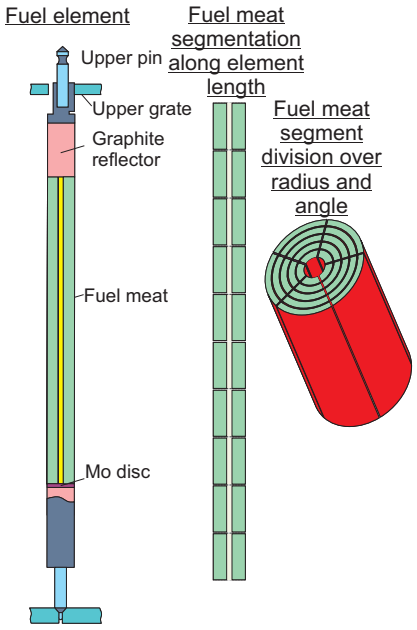

Figure 6: Fuel element fuel met division for delayed γ R2S calculation scheme.

The R2S methodology was applied to the U-ZrH part (fuel meat) of the fuel element, divided by a cylindrical mesh into 10 parts axially, 5 parts radially and 5 parts azimuthally (fig. 6). The aluminum box was placed as close as possible to the fuel rack, in order to evaluate the maximum gradient of the γ field, due to $\frac{1}{R^2}$ dependence, R being the distance from the sample to an individual fuel element.

The aim of these calculations was to determine the optimal choice and configuration of fuel elements in the rack in order to obtain the highest dose-rate or the most homogeneous field. The core is usually filled with 60 fuel elements during reactor operation, and up to 6 fuel elements can afterwards be transferred into the fuel rack, with numerous possible permutations. To limit this, a symmetric rack filling pattern was assumed, since the irradiation box is positioned symmetrically with respect to the fuel element rack. 4 representative fresh fuel elements, each from a separate core annulus were chosen (fig. 2) for delayed γ simulations. The aluminum box was modeled to the close position 0.5 cm from the rack frame, with the box bottom plate being located 8 cm below the fuel center height.

Since each individual fuel element can be considered as an independent γ source, separate γ transport simulations were performed for each rack position and each representative fuel element, and the results joined according to the chosen rack permutation. Reactor operation of 1 h at full power is simulated, and simulations of the delayed γ field performed 20 min after reactor shut-down, which is the minimum time needed for neutron decay and for transporting the elements to the fuel rack, without activating the fuel element grappler mechanism, and moving the irradiation box into position. Ambient dose equivalents using ICRP-21 (ICRP) H*10 ambient dose equivalent and ANSI-ANS6.1.1.1977 (ANS6) H*10 ambient dose equivalent flux to dose conversion factors and air kerma were calculated on a 1 cm $\times$ 1 cm $\times$ 1 cm mesh inside the aluminum box, everywhere below 10 % statistical error. To evaluate the homogeneity of the field inside the box, several homogeneity measures were calculated: $\frac{Max}{Min}$, $\frac{Max}{Ave}$ and $\frac{Max-Min}{Ave}$, where Max, Min and Ave are maximum, minimum and average field values respectively. The aim was to find a fuel element configuration, producing the most homogeneous field inside the box. All the available permutations were tested and the most optimal configuration (fig. 7a) was found. The configuration producing the strongest field inside the box consists only of B-ring fuel elements, since they are closest to the core center.

Fig. 7 displays the ICRP-21 H*10 ambient dose equivalent field inside the aluminum irradiation box at the fuel element center height. We can observe the configuration composed of E5 an B2 elements, producing a much more homogeneous field, comparing to the configuration composed of only B2 elements, which produces the highest intensity field. The shapes of both ANSI-ANS6.1.1.1977 H*10 ambient dose equivalent and air kerma fields are practically identical to the ICRP-21 H*10 ambient dose equivalent field, but scaled and offset according to tables 2 and 3.

Even though high dose rate gradients inside the irradiation box exist, the dose-rate is

Table 2: Homogeneity norms for most homogeneous (fig. 7a) configuration, after 1 h element irradiation and 20 min cool-down.

	Max	$\frac{Max}{Min}$	$\frac{Max}{Ave}$	$\frac{Max-Min}{Ave}$
H*10 ICRP [Sv h^{-1}]	$45.03(1 \pm 1 \times 10^{-2})$	$9.01(1 \pm 8 \times 10^{-2})$	$2.29(1 \pm 4 \times 10^{-2})$	$2.03(1 \pm 5 \times 10^{-2})$
H*10 ANS6 [Sv h^{-1}]	$53.05(1 \pm 1 \times 10^{-2})$	$8.11(1 \pm 7 \times 10^{-2})$	$2.23(1 \pm 3 \times 10^{-2})$	$1.95(1 \pm 4 \times 10^{-2})$
Air kerma [Gy h^{-1}]	$40.65(1 \pm 1 \times 10^{-2})$	$9.07(1 \pm 9 \times 10^{-2})$	$2.29(1 \pm 4 \times 10^{-2})$	$2.04(1 \pm 5 \times 10^{-2})$

Table 3: Homogeneity norms for highest intensity configuration (fig. 7b), after 1 h element irradiation and 20 min cool-down.

	Max	Max/Min	Max/Ave	$(Max-Min)/Ave$
H*10 ICRP [Sv h^{-1}]	$70.75(1 \pm 1 \times 10^{-2})$	$10.10(1 \pm 7 \times 10^{-2})$	$2.53(1 \pm 3 \times 10^{-2})$	$2.28(1 \pm 4 \times 10^{-2})$
H*10 ANS6 [Sv h^{-1}]	$83.30(1 \pm 1 \times 10^{-2})$	$9.11(1 \pm 6 \times 10^{-2})$	$2.47(1 \pm 3 \times 10^{-2})$	$2.20(1 \pm 3 \times 10^{-2})$
Air kerma [Gy h^{-1}]	$63.87(1 \pm 1 \times 10^{-2})$	$10.16(1 \pm 7 \times 10^{-2})$	$2.54(1 \pm 3 \times 10^{-2})$	$2.29(1 \pm 4 \times 10^{-2})$

still of the orders of 10 Sv h^{-1} or 10 Gy h^{-1}, even though fresh fuel and reactor operation of 1 h are considered. Increasing the reactor operation time to few hours, prior to moving the fuel elements into the rack would almost linearly increase the dose rate. Should the need for increased homogeneity at the expense of dose rate arise, the irradiation box could be moved further away from the rack. Further investigation on dose rate sensitivity to reactor operation time and irradiation box positions is required.

Since experimental dose mapping inside the irradiation box using TLD is planned, a new set of simulations will be performed, to reflect the experimental conditions and validate the computational scheme.

4 Conclusion

This paper presents the characterization of the gamma field inside the existing and a newly constructed irradiation facility in the JSI TRIGA reactor, due to the increased utilization of the reactor for pure γ irradiations.The prompt γ field inside the reactor existing irradiation facilities has been calculated, which together with previous γ profile measurements give an overview of the total γ field flux. The data will be utilized for detector choice during the γ field measurement campaign, during which special effort in discriminating the prompt and delayed γ field contributions. This data will serve for validation of a generalized delayed γ field R2S methodology computational code currently under development at JSI, which will be capable of simulating the delayed γ field with an arbitrary energy resolution, with other secondary particles (e.g. e^-,e^+,α). The code will afterwards routinely be used for characterization of the γ field in the irradiation facilities of the JSI TRIGA reactor in support of experimental campaigns and may later on be applied for radioactive waste qualification in the scope of decommissioning of the reactor.
The fuel element specific R2S computational scheme has been used to calculate the dose rate field inside a new, larger irradiation facility which utilizes activated fuel elements as a γ source. With initial measurements, taken in uncontrolled conditions and simulation data being of the same order of magnitude, a more thorough analysis is required to validate it. An experimental campaign for dose rate gradient measurements inside the irradiation box is planned in order to asses the methodology accuracy.
With JSI TRIGA irradiation facilities γ field qualification, and proposed optimization in terms of increasing the γ field intensity or homogeneity, we aim to accommodate a variety of samples for γ irradiation, ranging from material samples for γ heating assessment to whole electronic assemblies testing for aerospace, nuclear and particle accelerator

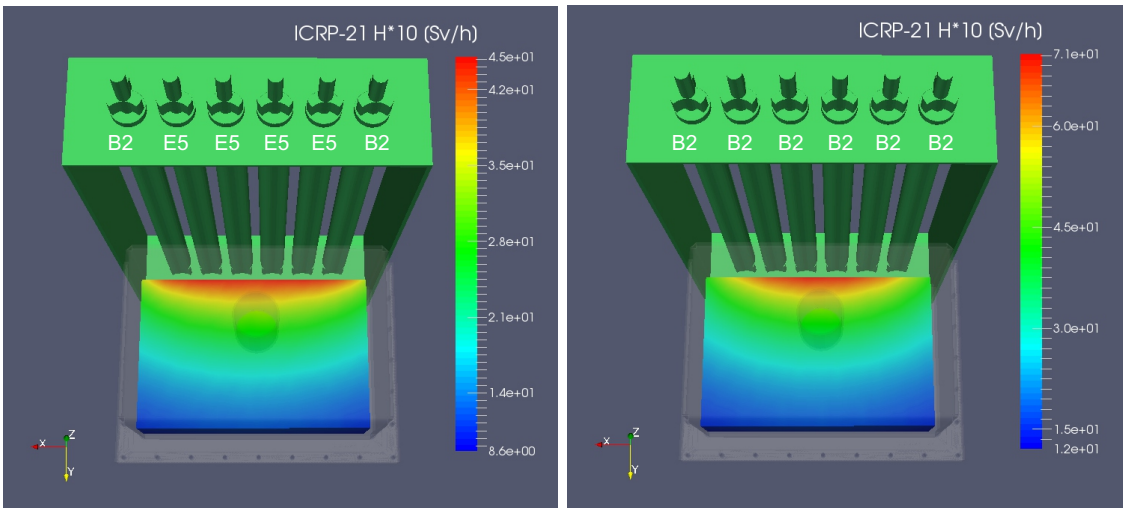

(a) Element configuration producing most homogeneous field.

(b) Element configuration producing most intense field.

Figure 7: ICRP-21 H*10 γ dose rate field at fuel element center line height, 20 min after reactor shut down.

technologies.

References

[1] C. W. Lee, C. H. Shin, and J. K. Kim. High-level radiation field analysis using Monte Carlo simulation in KORI nuclear power plant unit 1. In *Proceedings of the KNS autumn meeting*. KNS, 2003.

[2] Andrej Žohar and Luka Snoj. Analysis of the primary water activation in a typical PWR. In *25th International Conference Nuclear Energy for New Europe: Conference Proceedings*. Nuclear Society of Slovenia, 2016.

[3] Klemen Ambrožič and Luka Snoj. Delayed Gamma Ray Modeling Around Irradiated JSI TRIGA Fuel Element by R2S Method. In *25th International Conference Nuclear Energy for New Europe: Conference Proceedings*. Nuclear Society of Slovenia, 2016.

[4] R. E. Sharp and S. L. Pater. A comparison of the effects of gamma radiation from spent fuel and cobalt-60 on electronic components. In *RADECS 93. Second European Conference on Radiation and its Effects on Components and Systems (Cat. No.93TH0616-3)*, pages 48–55, Sep 1993.

[5] Luka Snoj, Gašper Žerovnik, and Andrej Trkov. Computational analysis of irradiation facilities at the JSI TRIGA reactor. *Applied Radiation and Isotopes*, 70(3):483 – 488, 2012.

[6] Gašper Žerovnik, Tanja Kaiba, Vladimir Radulović, Anže Jazbec, Sebastjan Rupnik, Loïc Barbot, Damien Fourmentel, and Luka Snoj. Validation of the neutron and gamma fields in the JSI TRIGA reactor using in-core fission and ionization chambers. *Applied Radiation and Isotopes*, 96:27–35, 2015.

[7] Igor Mandić, Vladimir Cindro, Andrej Gorišek, Gregor Kramberger, and Marko Mikuž. Online integrating radiation monitoring system for the ATLAS detector at the Large

Hadron Collider. *IEEE Transactions on Nuclear Science*, 54(4):1143–1150, Aug 2007.

[8] John Hale. Data for Protection Against Ionizing Radiation from External Sources: Supplement to ICRP Publication 15. ICRP Publication 21. By The International Commission on Radiological Protection. paper, pp.100, Elmsford, N.Y., Pergamon Press, 1973. *Radiology*, 111(3):716–716, jun 1974.

[9] ANS-6.1.1 Working Group, M. E. Battat (Chairman). American National Standard Neutron and Gamma-Ray Flux-to-Dose Rate Factors: ANSI/ANS-6.1.1-1977 (N666). Technical report, American Nuclear Society, 1977.

[10] D. Fourmentel, V. Radulović, L. Barbot, J. F. Villard, G. Žerovnik, L. Snoj, M. Tarchalski, K. Pytel, and F. Malouch. Delayed Gamma Measurements in Different Nuclear Research Reactors Bringing Out the Importance of Their Contribution in Gamma Flux Calculations. *IEEE Transactions on Nuclear Science*, 63(6):2875–2879, Dec 2016.

[11] Andrew Davis. *Radiation Shielding of Fusion Systems*. PhD thesis, University of Birmingham, 2010.

[12] Federico Ravotti. *Development and Characterization of Radiation Monitoring Sensors for High Energy Physics Experiments of the CERN LHC Accelerator*. PhD thesis, L'UNIVERSITE MOTPELLIER II, November 2006.

[13] John T. Goorley, Michael R. James, Thomas E. Booth, Forrest B. Brown, Jeffrey S. Bull, Lawrence J. Cox, Joe W. Jr. Durkee, Jay S. Elson, Michael Lorne Fensin, Robert A. III Forster, and et al. *Initial MCNP6 Release Overview - MCNP6 version 1.0*. Los Alamos National Laboratory (LANL), Jun 2013. Report number: LANL Report LA-UR-13-22934.

[14] M.B. Chadwick, P. Obloinský, M. Herman, N.M. Greene, R.D. McKnight, D.L. Smith, P.G. Young, R.E. MacFarlane, G.M. Hale, S.C. Frankle, A.C. Kahler, T. Kawano, R.C. Little, D.G. Madland, P. Moller, R.D. Mosteller, P.R. Page, P. Talou, H. Trellue, M.C. White, W.B. Wilson, R. Arcilla, C.L. Dunford, S.F. Mughabghab, B. Pritychenko, D. Rochman, A.A. Sonzogni, C.R. Lubitz, T.H. Trumbull, J.P. Weinman, D.A. Brown, D.E. Cullen, D.P. Heinrichs, D.P. McNabb, H. Derrien, M.E. Dunn, N.M. Larson, L.C. Leal, A.D. Carlson, R.C. Block, J.B. Briggs, E.T. Cheng, H.C. Huria, M.L. Zerkle, K.S. Kozier, A. Courcelle, V. Pronyaev, and S.C. van der Marck. Endf/b-vii.0: Next generation evaluated nuclear data library for nuclear science and technology. *Nuclear Data Sheets*, 107(12):2931 – 3060, 2006.

[15] R. Jeraj and M. Ravnik. Reactor U(20)–zirconium hydride fuel rods in water with graphite reflector, international handbook of evaluated criticality safety benchmark experiments. Technical report, NEA/NSC/DOC/(95) 03/III, 1999.

[16] Barbara Obryk, Paola Batistoni, Sean Conroy, Brian D. Syme, Sergey Popovichev, Ion E. Stamatelatos, Theodora Vasilopoulou, and Pawe Bilski. Thermoluminescence measurements of neutron streaming through JET Torus Hall ducts. *Fusion Eng. Des.*, 89(9-10):2235–2240, 2013.